PHYSICAL REVIEW E, VOLUME 63, 065204(R)

Subharmonic destruction of generalized chaos synchronization

Nikolai F. Rulkov[1] and Clifford Tureman Lewis[1,2]
[1]*Institute for Nonlinear Science, University of California, San Diego, La Jolla, California 92093-0402*
[2]*Department of Physics, University of California, San Diego, La Jolla, California 92092*
(Received 19 September 2000; revised manuscript received 6 February 2001; published 29 May 2001)

A bifurcation of transition that destroys generalized chaos synchronization is considered. This transition frequently occurs in regimes of subharmonic chaos entrainment where synchronization can be abruptly terminated due only to an almost unnoticeable change in the shape of the driving attractor. We explore the main cause of this sensitivity and ascertain the mechanism behind this transition.

DOI: 10.1103/PhysRevE.63.065204 PACS number(s): 05.45.Xt, 64.60.Cn

Chaos synchronization has emerged as an important and fundamental phenomenon with application in such diverse subjects as biological, neurological, laser, electrical, and fluid mechanical systems [1]. Accordingly, there has been great progress in formalizing a theory of *identical* synchronization [2] (identical systems that exhibit identical chaotic evolution). However, there is still much ongoing work towards formalizing a theory for the larger, overall class called *generalized* synchronization (two dissimilar coupled systems that undergo different chaotic evolution), which was conceptually introduced in Ref. [3]. The onset of generalized synchronization in directionally coupled chaotic systems corresponds to the formation of a continuous mapping that transforms the trajectory on the attractor of the drive system into the trajectory of the response system.

Significant progress has been made in defining criteria, which when satisfied, indicates that the synchronization mapping is differentiable and forms a normally hyperbolic manifold [4]. This differentiable generalized synchronization requires a strong contraction rate in the response system that overcomes the contraction rate in the drive system, and therefore this regime is spatially segregated from the critical states where one normally anticipates the loss of synchronization, e.g., the chaotic trajectories and/or the unstable periodic orbits (UPOs) become conditionally unstable [2,5]. Studies of the generalized synchronization of chaos in the entire range of the synchronization zone must deal with nondifferentiable continuous synchronization mappings. These mappings have rather complicated form and can behave differently depending upon the regime of synchronization. In this Rapid Communication we show that these mappings can have properties that bring about the sudden destruction of generalized chaos synchronization.

The characteristic feature of this regime of chaos synchronization is that the synchronization tolerates significant variations in the coupling strength and parameter values of the response system, but is susceptible to a small change in the dynamics of a driving system. For this regime almost unnoticeable change in the chaotic behavior of the drive system is able to completely destroy the synchrony between the systems, even when all response Lyapunov exponents are negative, and all the UPOs one would find in the synchronization regime remain conditionally stable. Since this transition is not due to bifurcations that destabilize some of the conditionally stable UPOs, it differs from the well-known *blowout* and *bubbling* transitions (see, for example, Ref. [5]). Our studies indicate that this transition frequently occurs in coupled chaotic oscillators synchronized in a chaotic regime with different fundamental frequencies.

To be more specific, we build our discussion based upon the results of numerical simulations of the regime of chaos synchronization with frequency ratio 2:1, which was previously observed in experiments with two electrical chaotic circuits [6]. The dynamics of the drive circuit are described by the set of differential equations of the form [6]

$$\begin{aligned} \nu\dot{x}_1 &= x_2, \\ \nu\dot{x}_2 &= -x_1 - \delta x_2 + x_3, \\ \nu\dot{x}_3 &= \gamma(\alpha_1 f(x_1) - x_3) - \sigma x_2. \end{aligned} \tag{1}$$

The response system equations are

$$\begin{aligned} \dot{y}_1 &= y_2, \\ \dot{y}_2 &= -y_1 - \delta y_2 + y_3, \\ \dot{y}_3 &= \gamma(\alpha_2 f(y_1) - y_3 + g x_1) - \sigma y_2, \end{aligned} \tag{2}$$

where g is the coupling strength, and $\gamma = 0.294$, $\sigma = 1.52$, $\delta = 0.534$, and $\alpha_2 = 16.7$ are fixed system parameters. The nonlinear function $f(x)$ models the input-output characteristics of a nonlinear converter in the circuit [7]. The parameter ν in the drive system equations is the time scaling parameter that is used to select the desired frequency ratio of the synchronization.

The phenomenon discussed in this paper is illustrated in Fig. 1. The values of the parameters in the drive and response systems are selected in a such way that both systems, when uncoupled, generate chaotic oscillations. The chaotic attractor in the driving system, with $\alpha_1 = 15.93$, is shown in Fig. 1(a). The attractor of the response system has a very similar form, but because of the parameter ν, the phase velocity of the trajectories of the driving attractor is about twice the size of the phase velocity in the response attractor trajectories. We set the values of $g = 3.0$ and $\nu = 0.498$, which corresponds to a point on the parameter plane (ν, g), which is about in the middle of the synchronization zone with frequency ratio 2:1 when the response system is driven by the trajectories of the chaotic attractor shown in Fig. 1(a). A Lissajous figure of this synchronous chaotic attractor is

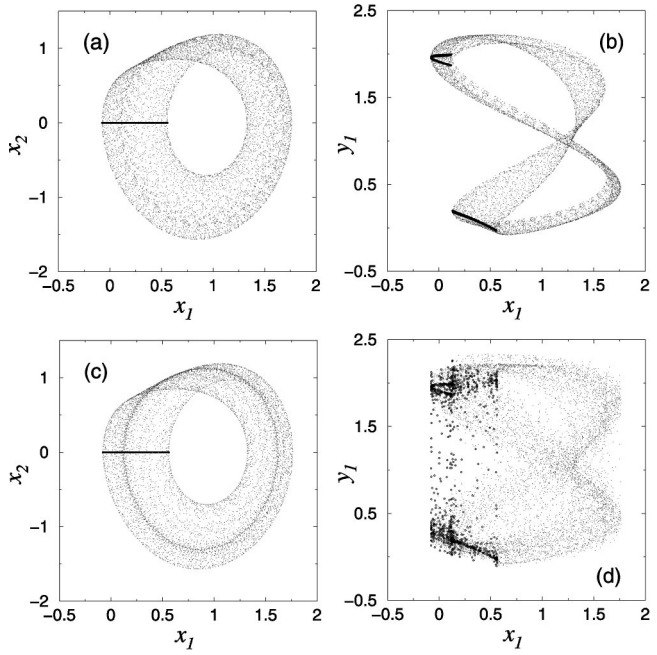

FIG. 1. Chaotic attractors of the drive system (left) computed for $\alpha_1=15.93$ (a) and $\alpha_1=15.94$ (c), along with Lissajous figures constructed from the drive and response attractors and plotted for (x_1,y_1) [$\alpha_1=15.93$ (b) and $\alpha_1=15.94$ (d)]. In both cases, all of the system parameter values are the same, except for α_1. The trajectories' intersections with the Poincaré cross section ($x_2=0$) are shown as bold dots.

shown in Fig. 1(b). The bold points shown against the background of the chaotic attractors correspond to the points on the Poincaré cross section where the trajectories cross the value $x_2=0$ with positive values of dx_2/dt.

It follows from the Lissajous figure that synchronization between the drive and response systems has frequency ratio 2:1. This synchronization regime turns out to be very robust against variation of the parameter values in the response systems as well as variation of the coupling strength. Synchronization also remains stable for values of α_1 in the drive system that are lower than the one shown in Fig. 1(a) ($\alpha_1=15.93$). However, this regime of synchronization abruptly terminates after a very slight increase in the value of α_1 (less then 0.1%). The chaotic attractors that occur after the destruction of this synchronization are shown in Figs. 1(c) and 1(d). These figures are obtained with the same parameter values as before except for the new value of α_1, now $\alpha_1=15.94$. Comparing with the chaotic attractors in Fig. 1, one can see that while the small change in α_1 does not cause any noticeable change in the drive system attractor $\mathcal{A}_{DR}$, the synchronization of the response system is completely terminated. Why is this regime of synchronization so completely destroyed by an almost unnoticeable change in $\mathcal{A}_{DR}$, when it tolerates significant changes in both the response system and the value of the coupling parameter? To answer this question we analyze this minor change of the drive system and study how it destroys the synchronization.

The distinctive feature of $\mathcal{A}_{DR}$ for the domain of values of α_1 where the systems are synchronized is the existence of a

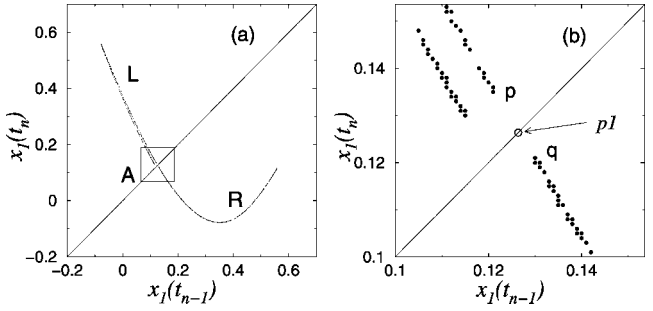

FIG. 2. Return map $(x_1(t_{n-1}),x_1(t_n))$, plotted for the trajectories of the drive system chaotic attractor $\mathcal{A}_{DR}$ with $\alpha_1=15.93$ (a) and the enlarged picture of the inset area A (b). t_n corresponds to the times when the chaotic trajectory crosses the Poincaré cross section $x_2=0$; see Fig. 1(a).

gap, which can be clearly seen in the return map shown in Fig. 2 as the interval between p and q. Due to the high dissipation in the drive system, this return map is almost a one-dimensional (1D) map. Approximating the dynamics on the attractor with the 1D map, one can split the map into two intervals: L (located on the left-hand side of the diagonal) and R (located on the right-hand side of the diagonal). Note that any trajectory, including chaotic trajectories and unstable periodic orbits (UPOs), of $\mathcal{A}_{DR}$ periodically alternates between the intervals L and R, changing intervals every iteration. We call such trajectories *uniformly alternating* trajectories.

It is clear from Fig. 2(b) that the periodic orbit of period 1 ($p1$), which is located between the intervals L and R, does not appear in the chaotic attractor $\mathcal{A}_{DR}$. When the value of α_1 increases to 15.94, the points p and q merge together. As the result, the orbit $p1$ now lies in the interior of the chaotic attractor $\mathcal{A}_{DR}$ and a new set of UPOs that contain nonuniform alternation of R and L, which have repetition of the same symbol in the sequence of Rs and Ls, are formed in the chaotic attractor. In this case the chaotic trajectory of $\mathcal{A}_{DR}$ is no longer a uniformly alternating trajectory.

Consider the features of the synchronization mapping that maps the chaotic trajectories and the UPOs of $\mathcal{A}_{DR}$ into the trajectories of the attractor in the response system. We computed all of the UPOs in the drive system up to period 6 and studied their respective response images that form limiting periodic orbits in the phase space of the response system. We computed both stable and unstable images, which, respectively, correspond to the conditionally stable and conditionally unstable UPOs in the drive-response system [9]. We index these images pN, where N stands for the period of the corresponding UPO in the phase space of the drive system. The Poincaré cross sections of the chaotic attractors, and the UPOs computed in the drive-response system are plotted on the plane (x_1,y_1) in Fig. 3.

Figure 3(a) presents the regime of synchronized oscillations, which is computed for the chaotic attractor shown in Figs. 1(a) and 1(b). In this case, the stable images for all of the UPOs of $\mathcal{A}_{DR}$ (indicated by open symbols) are mapped inside the synchronized chaotic attractor (which is plotted with circles). Figure 3(a) shows only the UPOs with $N\leqslant 6$. The unstable images for the same UPOs (they are indicated

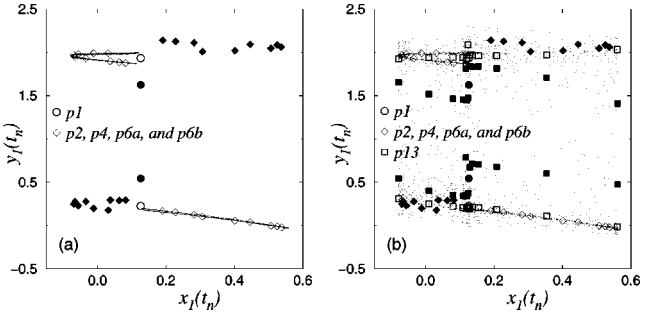

FIG. 3. The (x_1,y_1)-projections of the chaotic attractors (circles) and the UPOs (symbols) computed on the Poincaré cross section in the regime of synchronization with $\alpha=15.93$ (a) and asynchronous regime with $\alpha=15.94$ (b). Open (closed) symbols correspond to the UPOs that have stable (unstable) response images when the response system is driven by the UPOs of the drive system.

by closed symbols) are located well outside the chaotic attractor. While $\mathcal{A}_{DR}$ contains only uniformly alternating orbits, this separation of the regions with stable and unstable images is persistent. The stable image of the period-1 orbit, $p1$ (indicated by an open circle), is also outside the attractor. Note that although the trajectories of $\mathcal{A}_{DR}$ get very close to the period-1 orbit [see the projection of $p1$ onto the $x_1(t_n)$ axis], the coordinates of the stable image of $p1$ in the response systems are shifted a bit from the synchronized attractor [see the projection of the $p1$ image onto the axis $y_1(t_n)$]. The existence of this shift indicates that the synchronization mapping will experience dramatic changes once the period-1 orbits appears in the interior of $\mathcal{A}_{DR}$ as α_1 increases.

It is important to mention that the uniformly alternating UPOs map into the phase space of response system with a 1:1 mapping; see Fig. 3(a). When the systems are synchronized, the chaotic attractor $\mathcal{A}_{DR}$ contains only uniformly alternating orbits, and therefore, this regime of chaos synchronization is characterized by a 1:1 continuous mapping for *all* trajectories. This fact is also confirmed using the auxiliary system method [8]. Note that, although the synchronization mapping in this case is 1:1, the ratio of fundamental frequencies in this regime is 2:1.

Figure 3(b) presents the UPOs and chaotic attractor computed for the case when the synchronization is terminated due to a very small increase in α_1, as is shown in Figs. 1(c) and 1(d). Comparing Figs. 3(a) and 3(b), one can see that while the responses to the uniformly alternating UPOs (indicated by diamonds) experience negligible change, the synchronization mapping is completely destroyed. This destruction of the mapping is also confirmed with the auxiliary system method. We argue that the only reason for such an abrupt destruction is the appearance of the nonuniformly alternating UPOs inside $\mathcal{A}_{DR}$. These UPOs are born in the homoclinic structure formed by the stable and unstable manifolds of the $p1$ orbit. Due to the strong dissipation in our case, this homoclinic structure forms immediately before the points p and q merge together; see Fig. 2. Therefore, the first nonuniformly alternating UPO appears inside $\mathcal{A}_{DR}$ immediately before this bifurcation.

We have found that all of nonuniformly alternating UPOs are mapped into the phase space of the response system with a 1:2 mapping. As a result, the stable images each of these UPOs appear in both the region of stable and the region of unstable images for uniformly alternating UPOs; see Fig. 3(b). The complete set of UPOs form a skeleton of a chaotic attractor, and any chaotic trajectory can be considered as a trajectory that wanders among these saddle periodic orbits. Therefore in our case, when the chaotic trajectory of the drive system gets close to the nonuniformly alternating trajectory, it is dragged into the region of unstable images of the uniformly alternating UPOs. This is the mechanism that makes the chaotic trajectory appear arbitrarily close to a conditionally unstable UPO and forms a new chaotic attractor that contains both conditionally stable and conditionally unstable UPOs. The appearance of these distinct sets of UPOs in the chaotic attractor leads to a nonhyperbolic situation (see Ref. [10] and references therein), which can be detected by the appearance of outbursts of nonidentical behavior in the response and auxiliary systems [8], because the chaotic response trajectory computed for this nonhyperbolic set becomes extremely sensitive to an arbitrary small noise.

The emergence of the nonuniformly alternating chaotic trajectories inside of $\mathcal{A}_{DR}$ results in the flipping of the phase of subharmonic components in the frequency spectrum of the chaotic driving signal. Since this fact reflects the major element causing the loss of synchronization, we call this desynchronization process the *subharmonic* transition.

In the example presented, the termination of the chaos synchronization is quite clear from the analysis of the attractors in the Poincaré cross section (see Figs. 2 and 3). However, this transition is not detectable with the standard analysis based upon the Lyapunov exponents. Indeed, the spectrum of Lyapunov exponents for the drive system is (0.325, 0.000, -3.541) for $\alpha_1=15.93$ and (0.343, 0.000, -3.559) for $\alpha_1=15.94$, while the spectra of conditional Lyapunov exponents are all negative values and are equal to $(-0.089,-0.731,-0.779)$ and $(-0.033,-0.763,-0.802)$, respectively. All of the periodic orbits embedded in the chaotic attractors of the driving system also have images that have negative maximal conditional Lyapunov exponents, both for synchronous *and* asynchronous oscillation regimes. Therefore, this border of chaos synchronization cannot be detected based completely on this kind of stability analysis and requires careful analysis of the mapping. We believe that this situation is quite typical for regimes of chaos synchronization with the frequency ratios other than 1:1. It may also be observed in systems where the chaotic attractor contains UPOs with distinct mean frequencies.

In conclusion, we would like to emphasize that when the considered type of transition occurs, the synchronization mapping for the chaotic trajectories gets destroyed, despite the fact that all of the unstable periodic orbits continue to have stable periodic images in the response system. In addition, the coordinates and the multipliers of these images can also remain unchanged through the transition. We believe that this observation brings a very important massage to research exploring the phenomenon of generalized synchroni

zation, because many recent studies rely on the fact that stable responses to the UPOs of the driving attractor do exist, to confirm the stability of the chaos synchronization (see, for example, Ref. [11]). Although such justification seems to be appropriate for studies of identical synchronization [2], it can lead to wrong conclusions pertaining to the situation where one deals with generalized synchronization of chaos and, in particular, with the case of subharmonic entrainment of chaotic oscillations.

The authors are grateful to H.D.I. Abarbanel, V.S. Afraimovich, L. Kocarev, and U. Parlitz for helpful discussions. This work was supported in part by U.S. Department of Energy (Grant No. DE-FG03-95ER14516) and the U.S. Army Research Office (MURI Grant No. DAAG55-98-1-0269).

[1] See special focus issues on chaos synchronization: IEEE Trans. Circuits Syst., Part 1, **44** (1997); Chaos **7** (1997), and references therein.

[2] L. M. Pecora *et al.*, Chaos **7**, 520 (1997); B. R. Hunt and E. Ott, Phys. Rev. Lett. **76**, 2254 (1996); P. Ashwin, J. Buescu, and I. Stewart, Nonlinearity **9**, 703 (1996); D. Gauthier and J. Bienfang, Phys. Rev. Lett. **77**, 1751 (1996).

[3] V. S. Afraimovich, N. N. Verichev, and M. I. Rabinovich, Radiophys. Quantum Electron. **29**, 747 (1986); N. F. Rulkov, M. M. Sushchik, L. S. Tsimring, and H. D. I. Abarbanel, Phys. Rev. E **51**, 980 (1995); L. M. Pecora, T. M. Carroll, and J. F. Heagy, *ibid.* **52**, 3420 (1995); L. Kocarev and U. Parlitz, Phys. Rev. Lett. **76**, 1816 (1996).

[4] B. R. Hunt, E. Ott, and J. A. Yorke, Phys. Rev. E **55**, 4029 (1997); K. Josic, Phys. Rev. Lett. **80**, 3053 (1998).

[5] E. Ott and J. C. Sommerer, Phys. Lett. A **188**, 39 (1994); P. Ashvin, J. Buescu, and I. N. Stewart, *ibid.* **193**, 126 (1994); Sh. C. Venkataramani, B. R. Hunt, and E. Ott, Phys. Rev. E **54**, 1346 (1996); E. Barreto *et al.*, Phys. Rev. Lett. **84**, 1689 (2000).

[6] N. F. Rulkov, Chaos **6**, 262 (1996).

[7] In the numerical simulations, we modeled the function $f(x)$ with the formulas

$$f(x)=\mathrm{sgn}(x)(a-\sqrt{[d(f_p(x)-a)^2+c}]/d,$$

where

$$f_1(x)=\begin{cases}|x| & \text{if } |x|\leqslant a\\ -q(|x|-p) & \text{if } a<|x|\leqslant b\\ -a & \text{if } |x|>b.\end{cases}$$

$d=(a^2-c)/a^2$, $q=2a/(b-a)$, and $p=(b+a)/2$. The values of the parameters a, b, and c are chosen to be equal to 0.5, 1.8, and 0.03, respectively. See Ref. [6] for details.

[8] H. D. I. Abarbanel, N. F. Rulkov, and M. M. Sushchik, Phys. Rev. E **53**, 4528 (1996).

[9] L. M. Pecora and T. L. Carroll, Phys. Rev. Lett. **64**, 821 (1990).

[10] T. Sauer, C. Grebogi, and J. Yorke, Phys. Rev. Lett. **79**, 59 (1997); E. Barreto and P. So, *ibid.* **85**, 2490 (2000).

[11] U. Parlitz, L. Junge, and L. Kocarev, Phys. Rev. Lett. **79**, 3158 (1997).